

WSRT ULTRA-DEEP NEUTRAL HYDROGEN IMAGING OF GALAXY CLUSTERS AT Z≈0.2, A PILOT SURVEY OF ABELL 963 AND ABELL 2192

MARC VERHEIJEN¹, J.H. VAN GORKOM², A. SZOMORU³, K.S. DWARAKANATH⁴, B.M. POGGIANTI⁵, AND D. SCHIMINOVICH²

Draft version June 18, 2018

ABSTRACT

A pilot study with the powerful new backend of the Westerbork Synthesis Radio Telescope (WSRT) of two galaxy clusters at $z=0.2$ has revealed neutral hydrogen emission from 42 galaxies. The WSRT probes a total combined volume of 3.4×10^4 Mpc³ at resolutions of 54×86 kpc² and 19.7 km/s, surveying both clusters and the large scale structure in which they are embedded. In Abell 963, a dynamically relaxed, lensing Butcher-Oemler cluster with a high blue fraction, most of the gas-rich galaxies are located between 1 and 3 Mpc in projection, northeast from the cluster core. Their velocities are slightly redshifted with respect to the cluster, and this is likely a background group. None of the blue galaxies in the core of Abell 963 are detected in H I, although they have similar colors and luminosities as the H I detected galaxies in the cluster outskirts and field. Abell 2192 is less massive and more diffuse. Here, the gas-rich galaxies are more uniformly distributed. The detected H I masses range from 5×10^9 to 4×10^{10} M_⊙. Some galaxies are spatially resolved, providing rudimentary rotation curves useful for detailed kinematic studies of galaxies in various environments. This is a pilot for ultra-deep integrations down to H I masses of 8×10^8 M_⊙, providing a complete survey of the gas content of galaxies at $z=0.2$, probing environments ranging from cluster cores to voids.

Subject headings: galaxy clusters: general — galaxy clusters: individual(Abell 963, Abell 2192)

1. INTRODUCTION

It has long been recognized that the morphological mix of galaxy types is very different in the centers of clusters than in the field. Ellipticals and S0's dominate in dense clusters, spirals and irregulars dominate elsewhere. More recent studies have shown that the galaxy population of clusters at intermediate redshifts evolves over relatively short timescales. Beyond $z \approx 0.2$, clusters have a larger fraction of blue galaxies, indicative of ongoing star formation; the so called Butcher-Oemler (B-O) effect (Butcher and Oemler, 1978). The morphological mix in clusters also changes with redshift. Although the fraction of ellipticals remains unchanged from $z=1$ to 0, distant clusters have a significant fraction of spirals and hardly any S0's, while this situation is reversed for more nearby clusters (Dressler et al 1997, Fasano et al 2000, Lubin, Oke & Postman 2002). Furthermore, recent data from the local universe suggests there are smooth gradients in star formation rate, gas content and morphological mix, out to several Mpc from the cluster centers (Goto et al 2003; Balogh et al 1998; Solanes et al 2001). More specifically, there is an ongoing debate whether it is the cluster environment that drives the morphological evolution of galaxies or whether it is the accreted field population that evolves with redshift. In a study of a classic B-O cluster at $z=0.6$, Tran et al (2005) find that the blue

starforming galaxies are predominantly associated with an infalling structure, thus providing a strong argument that the B-O effect is linked with infall.

Despite all these data, nothing much is known about the cold neutral **gas** content of galaxies beyond $z=0.08$. The gas content is a critical parameter in environmentally driven galaxy evolution, since cold gas forms the reservoir of fuel for star formation, and the extended cold gas disks are sensitive tracers of tidal and hydrodynamical interactions. The main impediments to observe H I in galaxies at larger redshifts are the necessarily long integration times and man-made interference outside the protected 21cm band. So far, H I emission has been detected from only one galaxy at $z=0.176$ (Zwaan, van Dokkum & Verheijen, 2001). Nevertheless, if one were to sample a large volume and observe many galaxies at once, it would be worth the long integration time.

Radio synthesis telescopes, with their large field of view and sufficient angular resolution to resolve individual galaxies, are the ideal instruments for this. However, one drawback of synthesis instruments has been the limited instantaneous velocity coverage, typically no more than 2000 km/s, which is insufficient to cover the range of velocities usually seen in clusters (up to 5000 km/s). This has now changed with the new backend of the WSRT. In a single pointing, 18,000 km/s can be covered with sufficient velocity resolution, probing not only the entire velocity range of the cluster but also a very significant volume in front of and behind the cluster. Such an observation would provide the gas content of all galaxies in the cluster and the surrounding large scale structure. Here, we report on first results from a pilot study for just such a survey.

Two clusters were selected, known to be very different in their dynamical state and star formation properties. **Abell 963**, at $z=0.206$, has a velocity dispersion of 1350 km/s and is one of the nearest B-O clusters with a high

¹ Kapteyn Astronomical Institute, University of Groningen, PO Box 800, 9700 AV Groningen, The Netherlands;
 verheijen@astro.rug.nl

² Dept of Astronomy, Columbia University, 550 W 120th Street, New York, NY 10027, USA; ds@astro.columbia.edu,
 jvangork@astro.columbia.edu

³ Joint Institute for VLBI in Europe, Dwingeloo, The Netherlands; szomoru@jive.nl

⁴ Raman Research Institute, Sadashivanagar, Bangalore 560 080, India; dwaraka@rri.res.in

⁵ INAF - Padova Astronomical Observatory, Vicolo Osservatorio 5, 35122 Padova, Italy; poggianti@pd.astro.it

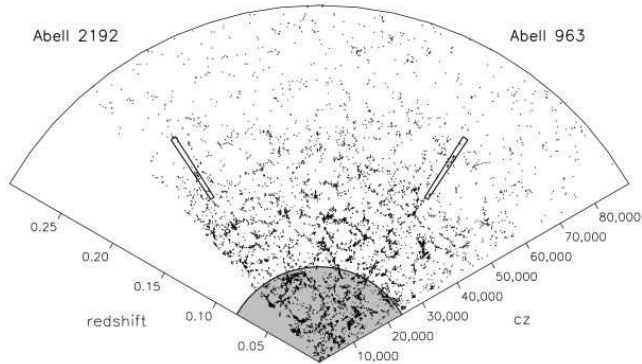


FIG. 1.— SDSS pie-diagram along a great circle passing through both clusters studied here. The grey area indicates the local volume in which clusters have been studied in H I so far. Boxes indicate the volumes surveyed by us in H I with the WSRT.

fraction (19%) of blue galaxies (Butcher et al 1983). This lensing X-ray cluster is unusually relaxed with less than 5% substructure (Smith et al 2005). **Abell 2192**, at $z=0.188$, has a velocity dispersion of 650 km/s and is much more diffuse. So far, it has not been detected in X-rays and the fraction of blue galaxies in this cluster has not yet been determined. Both clusters are observed by the Sloan Digital Sky Survey (SDSS). In Figure 1 we show a pie-diagram taken from the SDSS along a great circle passing through both clusters. The boxes indicate the volumes probed by the WSRT. Clearly, the clusters only occupy a tiny fraction of the volume. We also obtained deeper B- and R-band images for both clusters (Figure 2, Plate 1) and some optical redshifts for Abell 2192 with Hydra on WIYN at Kitt Peak. The box in Figure 2 indicates the area of A963 observed by Butcher et al (1983).

2. OBSERVATIONS

To prove the feasibility of observing the H I content of galaxies in and around these clusters with the WSRT, Abell 963 was observed for 20×12 hrs in February 2005, and Abell 2192 was observed for 15×12 hrs in July 2005. Each cluster was observed with a single pointing. The correlator was configured to give eight, partially overlapping, 10 MHz bands (IVC's) with 256 channels per band and 2 polarizations per channel. The frequency range covered is 1220–1160 MHz or $0.164 < z < 0.224$. After standard data reduction procedures, the data from all 8 IVCs were combined for each cluster into a single datacube comprising 1600 channel maps. The achieved typical rms noise levels per frequency channel are $68 \mu\text{Jy}/\text{beam}$ at 1178 MHz for A963, and $91 \mu\text{Jy}/\text{beam}$ at 1196 MHz for A2192. After Hanning smoothing, the rest-frame velocity resolution is 19.7 km/s while the synthesized beam is $17 \times 27 \text{ arcsec}^2$ or $54 \times 86 \text{ kpc}^2$ at 1190 MHz ($\Omega_M=0.27$, $\Omega_\Lambda=0.73$, $H_0=71 \text{ km/s/Mpc}$).

In search of H I emission, we further smoothed the data to a velocity resolution of 40 km/s and visually inspected both datacubes. Based solely on the H I datacubes, we identified 20 H I detections in the field of A963, and 30 in that of A2192. Subsequently, we queried the SDSS images for optical counterparts within the synthesized beam and found 19 objects for A963 and 23 for A2192. We consider these 42 H I detections as secure and the remaining 8 as tentative, given the shallowness of the SDSS. Unfortunately, SDSS spectroscopy, as an additional check,

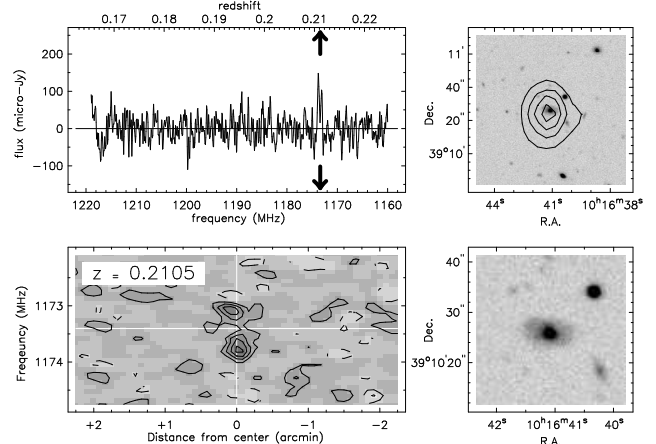


FIG. 3.— One example of our H I detections; a spatially resolved galaxy at the same redshift as Abell 963. Upper left: HI spectrum over the full velocity range. Arrows indicate the redshift (top) and observed frequency (bottom) of the H I emission. Lower left: position-velocity diagram extracted from the H I datacube, taken along the major axis of the galaxy. The horizontal white line indicates the systemic velocity. The vertical white line coincides with the spatial center of the galaxy. Upper right: integrated H I map in contours overlaid on an R-band image in grayscales. Lower right: blow-up of the optical image, showing the morphology of a normal spiral galaxy.

is only available for one of our H I detections. Assuming that the surveyed volume (Figure 1) is representative of the local Universe at large, in terms of galaxy density distributions, allows us to compare our H I detection rate with those obtained in blind H I surveys at lower redshifts. Given the local H I mass function (Zwaan et al 2003), the surveyed volume, the achieved noise levels, and an equivalent detection threshold of 4 sigma in 3 resolution elements, the predicted number of detectable galaxies is 22 for A963 and 17 for A2192. The detection rate in our pilot data is roughly as expected.

3. RESULTS

The quality of the data is exquisite. In Figure 3 we show typical data on an individual galaxy in the outskirts of Abell 963. The upper panel shows the double peaked profile. Although the total H I image, shown in the bottom left panel, seems barely resolved, the position velocity diagram taken along the photometric major axis shows that the kinematics helps to spatially resolve the galaxy. Its rudimentary rotation curve looks promising for future Tully-Fisher studies of galaxy samples in different environments at this redshift. Individual H I detections have H I masses between $5 \times 10^9 M_\odot$, close to our detection limit, and $4 \times 10^{10} M_\odot$.

In Figure 4 we show the redshift distributions of the H I detected galaxies compared to those of optically selected galaxies with optical redshifts. We identify the clusters with a velocity range of $\pm 3\sigma$ around the cluster mean velocity, where σ is the cluster velocity dispersion. This corresponds to $0.1897 < z < 0.2223$ for A963 and $0.1803 < z < 0.1957$ for A2192, as indicated by the horizontal bars. For A2192, half of the H I detections are outside this velocity range (dashed histogram) and are located at large projected distances from the cluster center. These are likely fore- and background galaxies. For A963, most of the H I detections are within the cluster velocity range but as we shall discuss below, many of those are likely to be background galaxies. Galaxies that

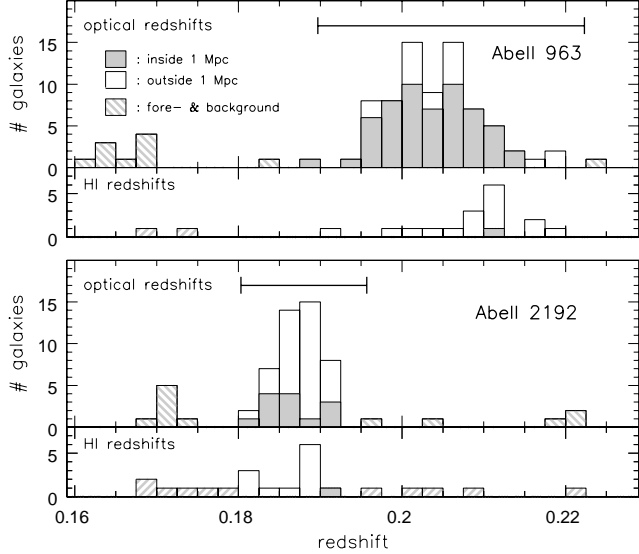


FIG. 4.— Redshift distributions of optically selected galaxies with optical redshifts in the upper panels, compared to those of H I detected galaxies in the lower panels. The adopted cluster redshift ranges are indicated by horizontal bars. Dashed histograms indicate fore- and background galaxies. Solid histograms indicate galaxies within 1 Mpc from the cluster centers, open histograms indicate galaxies outside 1 Mpc.

are located within a projected distance of 1 Mpc from the cluster centers are indicated with filled histograms and those outside 1 Mpc with open histograms. Cluster membership obviously depends on both, with an expected decreasing velocity range for cluster members at larger projected distances.

Figure 5 shows the distributions of galaxies on the sky with known redshifts within the velocity ranges of the clusters. Solid symbols indicate our H I detections while open symbols indicate optically selected galaxies with optical redshifts. To give a sense of scale, the small dotted circles have a radius of 1 Mpc at the distance of the clusters. The large dashed circles indicate the FWHM of the primary beam of the WSRT. Note that R_{200} is 3 Mpc and 1.5 Mpc for Abell 963 and Abell 2192 respectively. The field of view of the WSRT extends far beyond the clusters. Although the H I detection rate is quite similar for both regions, the spatial distributions of the H I detections are very different for the two clusters. The H I detected galaxies in the field of A963 are strongly clustered toward the northeast of the cluster, while the H I detected galaxies in A2192 appear to be more uniformly distributed over the surveyed area. For each cluster we only detect one galaxy within 1 Mpc from the center. The galaxies to the NE of A963 are also strongly clustered in velocity, centered near $z=0.21$ in Figure 4. Hence their mean velocity is redshifted by about 1200 km/s with respect to the cluster mean. Their mean projected distance from the cluster center is less than 2 Mpc. There is a velocity gradient from east to west of 2100 km/sec over approximately 4 Mpc at the distance of the cluster. This could be part of the filament seen in Figure 1 and is likely to be in the background to Abell 963.

We can ask whether the galaxies detected in HI differ in other ways from the non-detected galaxies. In Figure 6 we show, with identical symbols as in Figure 5, a combined color-magnitude diagram for both clusters with all the galaxies within their redshift ranges. Model magni-

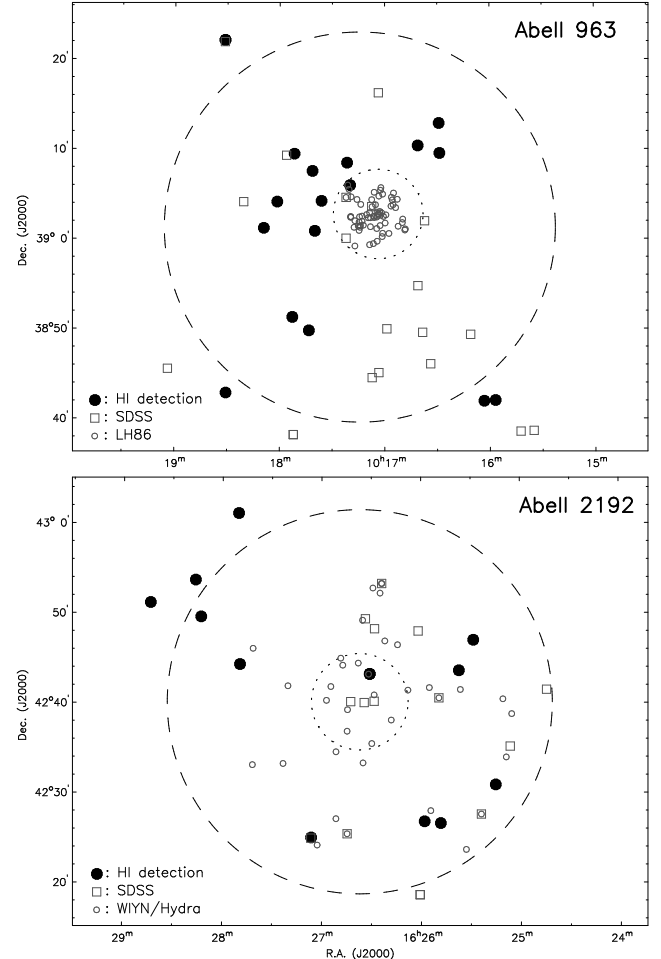


FIG. 5.— Sky distributions of galaxies with optical and H I redshifts within the velocity ranges of the clusters. Solid symbols: H I detected galaxies. Open squares: galaxies with optical SDSS redshifts. Open circles: galaxies with optical redshifts from Lavery & Henry (1986, LH86) for A963, and from our WIYN/Hydra spectroscopy for A2192. Small dotted circles have a radius of 1 Mpc at the distance of the clusters. Large dashed circles indicate the FWHM of the primary beam of the WSRT.

tudes from SDSS DR5 are used, corrected for Galactic extinction and k -corrected following Blanton & Roweis (2007). Absolute magnitudes are obtained by subtracting an effective distance modulus corresponding to the mean redshifts of the clusters. This figure clearly shows the red sequence characteristic of a cluster population as well as the 'blue cloud'. The main conclusion we can draw from Figure 6 is that our H I detected galaxies are in the same magnitude and color range as the non-detected blue galaxies within 1 Mpc from the center of A963 (most of the small circles in the blue cloud). This suggests that it is the location of the blue galaxies that determines the H I detection rate.

This result gets enhanced when we probe deeper by stacking the H I spectra of galaxies with known optical redshifts. We have done this separately for 12 blue galaxies within 1 Mpc of A963 with optical redshifts from Lavery and Henry (1986), and for 14 blue galaxies without an H I detection outside 1 Mpc in both fields. In Figure 7 we show the spectra for both samples (thick lines). As a control experiment we also show stacked spectra at 8 positions offset from the galaxies, but shifted to the same velocity (thin lines). There is no statistical detection of

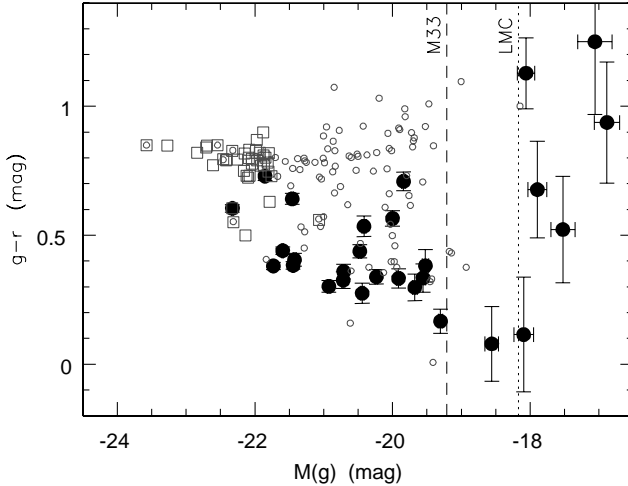


FIG. 6.— SDSS-based color-magnitude diagram for both clusters combined, including only galaxies with optical or H I redshifts within the cluster redshift ranges (see Fig. 4). Model magnitudes from SDSS DR5 are used, corrected for Galactic extinction and k -corrected following Blanton & Roweis (2007), but without internal extinction corrections. Absolute magnitudes are obtained by subtracting an effective distance modulus corresponding to the mean redshifts of the clusters. Symbols are identical to those in Figure 5. Dashed vertical lines indicate the magnitudes of M33 and the LMC.

the blue galaxies within 1 Mpc of A963. In contrast, the blue galaxies in the fields outside the central Mpc do show a statistical detection in the stacked H I spectra.

4. DISCUSSION

We present the results of a pilot study to demonstrate the feasibility of performing an H I emission line survey at $z=0.2$. Our detection rate and achieved noise levels show that it is now entirely feasible to do deep searches for H I in emission at cosmologically interesting distances and even obtain spatially resolved kinematics for individual galaxies. The preliminary results have interesting implications. While our detection rate is similar for both clusters, the distribution of the H I detections is more clustered for the dense and dynamically relaxed B-O cluster. The most noticeable result is that within the redshift range of A963 we detect 16 very gas-rich galaxies outside a radius of 1 Mpc from the cluster center, and only one just within that radius. At the same time we know that A963 has a significant fraction of blue galaxies in that central cluster region. Our stacked H I spectra suggest that the central blue galaxies have significantly smaller H I masses (on average) than similar blue galaxies outside the central Mpc. Since the H I detected galaxies are

of similar color and magnitude as the non-detected blue galaxies in the central region, we conclude that it is the location that matters. The central blue galaxies seem to have lost (a significant fraction of) their gas when they came to within 1 Mpc of the center of A963.

Our final survey will go down to an H I mass limit of $8 \times 10^8 M_{\odot}$. We expect to detect hundreds of galaxies in the clusters and in the large scale structure in which they are embedded. The survey goes out to 4 Mpc from the cluster centers in the plane of the sky (Figure 5), and covers a velocity range of 18,000 km/s (Figure 4), including filaments and voids (Figure 1). This will give the first optically unbiased H I survey at $z=0.2$ with enough sensitivity to detect even galaxies like the LMC in a volume similar to that of the entire local Universe out to 25 Mpc.

We thank R. Lavery for providing redshifts of galaxies in A963, T. Oosterloo and K. Kovač for providing the optical images of A963, and S. Trager for useful discussions. The WSRT is operated by the Netherlands Foundation for Research in Astronomy with support from the Netherlands Foundation for Scientific Research. The WIYN Observatory is a joint facility of the Universities of Wisconsin, Indiana and Yale, and the NOAO. This work benefitted from a NSF grant AST-06-07643 to Columbia University. This work used the Sloan Digital Sky Survey Archive. Its full acknowledgement is found at <http://www.sdss.org>.

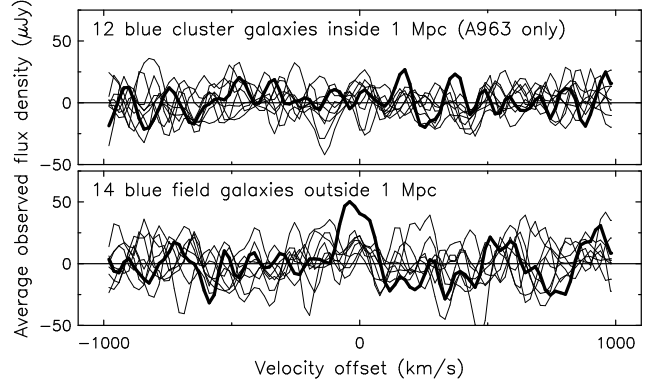


FIG. 7.— Stacked H I spectra of blue galaxies with optical redshifts, not detected individually in H I. Two different galaxy populations are considered. Top: blue B-O galaxies within 1 Mpc of the core of A963; bottom: blue galaxies in the field of A2192 outside 1 Mpc of the cluster core. Thin black lines indicate stacked spectra from 8 spatially offset positions.

REFERENCES

- Balogh, M.L., Schade, D., Morris, S., Yee, H.K.C., Carlberg, R.G., & Ellingson, E. 1998, ApJ, 504, L75
 Blanton, M.R. & Roweis, S. 2007, AJ, 133, 734
 Butcher, H., Wells, D.S. & Oemler, A. Jr. 1983, ApJS, 52, 183
 Butcher, H. & Oemler, A. Jr. 1978, ApJ, 219, 18
 Dressler, A. et al 1997, ApJ, 490, 577
 Fasano, G., Poggianti, B.M., Couch, W.J., Bettoni, D., Kjaergaard, P., & Moles, M. 2000, ApJ, 542, 673
 Goto, T., et al 2003, MNRAS, 346, 601
 Kodama, T., Smail, I., Nakata, F., Okamura, S., & Bower, R.G. 2001, ApJ, 562, L9
 Lavery, R.J. & Henry, J.P. 1986, ApJ, 304, L5
 Lubin, L.M., Oke, J.B., & Postman, M. 2002 AJ, 124, 1905
 Smith, G.P., Kneib, J.-P., Smail, I., Mazzotta, P., Ebeling, H., & Czoske, O. 2005, MNRAS, 359, 417
 Solanes, J.M., Manrique, A., Garcia-Gomez, C., Gonzalez-Casado, G., Giovanelli, R., & Haynes, M. 2001, ApJ, 548, 97
 Tran, K.-V., van Dokkum, P., Illingworth, G.D., Kelson, D., Gonzalez, A., & Franx, M. 2005, ApJ, 619, 134
 Zwaan, M., van Dokkum, P. & Verheijen, M. 2001, Science, 293, 1800
 Zwaan, M. et al 2003, AJ, 125, 2842

FIG. 2.— Plate (figure2.jpg) Optical images, 1.5×2 Mpc on a side, of the central regions of Abell 963 (top) and Abell 2192 (bottom). Colors are constructed from B- and R-band images taken with the Wide Field Camera on the Isaac Newton Telescope at La Palma for Abell 963, and with the NOAO Mosaic Camera on the 0.9m at Kitt Peak for Abell 2192. The color scales are slightly different for the two images. The area of A963 within which Butcher et al (1983) determined the fraction of blue galaxies, is indicated with a box.

This figure "figure2.jpg" is available in "jpg" format from:

<http://arxiv.org/ps/0708.3853v1>